

EFFECT OF LASER HARDENING ON THE PROPERTIES OF PM STEELS

Dušan Rodziňák¹⁾, Jozef Čerňan¹⁾, Rudolf Zahradníček¹⁾

¹⁾ Faculty of Aeronautics, Technical University Košice, Slovakia

Received: 25.03.2013

Accepted: 23.07.2013

Corresponding author: e-mail: dusan.rodzinak@tuke.sk, tel.: 00421 905 635 870, Faculty of Aeronautics, Technical University Košice, Slovakia, Rámpova 7, 04121 Košice

Abstract

The article deals with the influence of laser beams, which when acting on materials affect their surface. Depending on the intensity of exposure and the speed of displacement of the beam, due to the heating of the material and the subsequent cooling, there occurs the change in the pattern of the surface and of course to a change in the properties in the volume that was exposed to the temperature changes. For the tests the sintered material based on iron powder type Astaloy CrL and CrM containing 0.7% C was used. Results showed that by the appropriate combination of laser parameters it was possible to obtain the same structures as by using the technology of "sinterhardening". Compared to sintered state, the hardness of the surface of a material CrL +0.7% C values increased from 248 to 911 - 1000 and at material CrM +0.7% C values from 450 to 1043 - 1100 HV 0.05, depending on the velocity of displacement of the beam. The same is true for the values of microhardness. Hardness values reflect the structural changes that occur in the material due to rapid heating and subsequent rapid cooling. The first tests of this technology demonstrated its high variability and the potentials of replacing classical procedures.

Keywords: laser hardening, sintered material, structure, hardness

1 Introduction

Laser hardening is one of the new technologies, which is currently widely used in the manufacture of machine parts. The principle of laser quenching consists in the rapid heating of the material surface by laser, short holding time at temperature followed by cooling, heat dissipation due to thermal conductivity of the material.

A significant advantage of the heat treatment is its speed, quality and especially stable reproducibility. In addition, it provides low thermal load to the ambient material, minimum distortions, low surface oxidation and prevents formation of surface cracks. It is also possible to arrange for local hardening only at the desired location, to control the depth of hardening and the resulting hardness. The temperature is in many cases controlled on-line by a pyrometer directly integrated in the optics. Typical applications include local hardening of molds, tools, gears and racks, guide surfaces, parts of transmissions, shafts, cams and turbine blades and vanes [1- 5].

Nowadays, when in the engineering practice, powder metallurgy product are increasingly promoted, knowing the possibilities of using this type of heat treatment at this type steels is quite real. In the actual powder metallurgy practice in connection with the development of steels for highly stressed components, such alloyed materials has been introduced, which following heat treatment by hardening are able to achieve the desired mechanical properties. In addition to conventional quenching, by some suitably alloyed materials, there are currently method in use

called sinterhardening. In this case, at the accelerated regulated cooling directly from sintering temperature the hardening effect is achieved, i.e. formation of non-lamellar ferrite-carbide structure, whether of bainite or martensite nature. This sinterhardening effect is well known and well described in the literature, for example [6-12]. It appears that by this way it is possible to achieve a tensile strength of 1200 MPa by CrL type material and by CrM type material of 1400 MPa (with suitable carbon content, higher density and higher sintering temperature). How these PM materials act under the effect of laser beam is the content of this article.

2 Experimental conditions and materials

Samples were prepared from pre-alloyed steel powders from Höganäs company of types Astaloy CrL (Fe-1,5% Cr-0, 2% Mo) and Astaloy CrM (Fe-3% Cr-0, 5% Mo). Two sets of samples were created by adding graphite powder contents of 0.7%. After the addition of HWC type lubricant, samples were made compact under 600 MPa to form circular specimens of dimension $\phi 30 \times 5$ mm. Then they were sintered in controlled atmosphere (90% $N_2 + 10\% H_2$) at $1120^\circ C / 60$ min. The sintering atmosphere was frozen before sintering - dew point of $-57^\circ C$. Samples were placed into a retort with a mixture of Al_2O_3 with addition of 1% C to avoid possible undesirable oxidation and decarburization of sample surfaces. After sintering the samples were cooled outside the furnace in an inert atmosphere. Subsequently, they were machined on the outer diameter of $\phi 28$ mm with an internal hole of $\phi 10$ mm and finally polished to achieve flatness on both circular areas.

The special shape of the samples was made due to the fact that these samples were also used for contact fatigue testing and assumed for laser hardening.

All samples were subjected to laser hardening by diode-pumped solid-state laser system TRUMF TRUDISK serie 8002 under the following conditions. Samples were sprayed with matt black paint (paint hot Plasti-Kote industrial) resistant to higher temperatures to increase the absorption. Carrying beam was 2 kW, 4 mm diameter fiber. Progressive rate 25, 30, 40 mm/s was set only experimentally based on the experience of the external device operator. The process was controlled by constant beam power. Quenching was in a protective argon gas streaming at 15 l/min. Hardening took place on the sample surface in a single lane on one side and in two overlapping lanes on the other side of it, see - **Fig. 1a, b**.

The samples after tests were subjected to metallographic - microscopic analysis, hardness and micro-hardness measurements. Hardness values were determined by conventional tests such as the Vickers HV 10 and HV0.05.

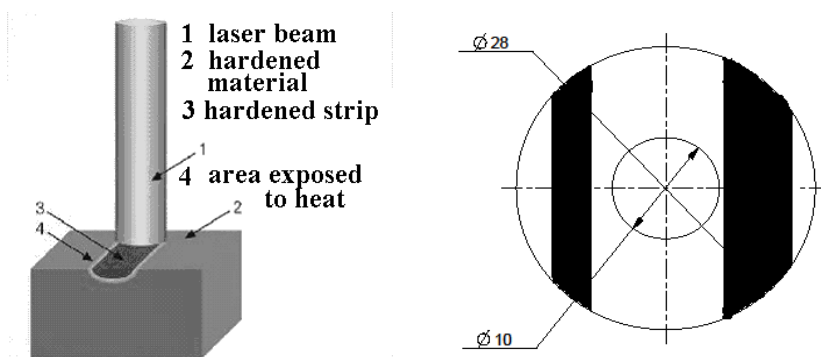


Fig.1a) Principle of laser hardening and **b)** hardened strips on the test specimen

3 Results and discussion

Tests were applied to these two material variants: **1- CrL**: Fe-1.5% Cr-0.2% Mo +0.7C and **2 – CrM**: Fe-3% Cr-0.5% Mo + 0.7C. Due to the fact that in the first place, we will address the impact of laser hardening on fundamental characteristics of the examined materials, it has been introduced in the **Table 1**. So there is the possibility of comparison with the results obtained following laser hardening.

Table 1 Characteristics of the investigated materials following sintering.

Material	CrL+0.7C	CrM+0.7C
Density ρ [g·cm ⁻³]	6.94	6.82
Porosity [%]	12	13.4
HV10	134	250
HV0.05	248	450

Based on microscopic analysis, in accordance with the transformation diagrams for the chemical composition, carbon content and cooling rate on microstructure is presented on **Figs. 2a, b**. Microstructure of samples Astaloy CrL + 0.7% C is composed mainly of fine pearlite and ferrite. In the case of Astaloy CrM + 0.7% C microstructure consists of bainite and ferrite and islands of very fine pearlite. More detailed analyzes of these base materials are listed in [13-15].

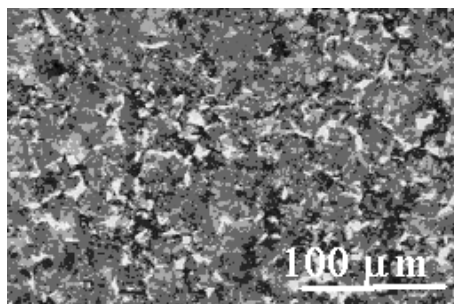


Fig.2 a Microstructure CrL + 0.7C

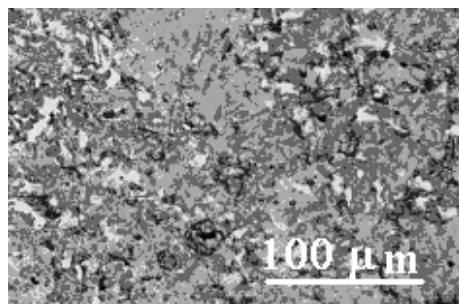


Fig. 2 b Microstructure CrM + 0.7C

Metallographic analysis of samples after laser hardening showed the following facts: the laser beam affects the surface of the sample in the form of spherical cymes in a certain width, which is set according to the needs and specifications of laser device. In our case, it represented about 4.5 mm. The depth of penetration into the material varies depending on the speed of a moving beam (at constant power of devices). To ensure that on the whole surface to get approximately the same depth of penetration into the material, that movement of the beam guided so that the individual tracks overlap. All this is evident from **Fig. 3**. Here are 3 practical and marked changes compared to the pure sintered state. Firstly, it is the affected area width and width of overlapping. These values, by constant technical parameter settings, do not change virtually. Therefore, next we will monitor only influence of the movement speed of the beam on the depth of penetration into the material, and the resulting changes in the structure or changes in hardness. As stated in the "Experiments", 3-speed movement - 25, 30, 40 mm /s were used. Their influence on depth of penetration into the material is shown in **Fig. 4a**. In this area structural changes occur, that ultimately affect the mechanical properties.

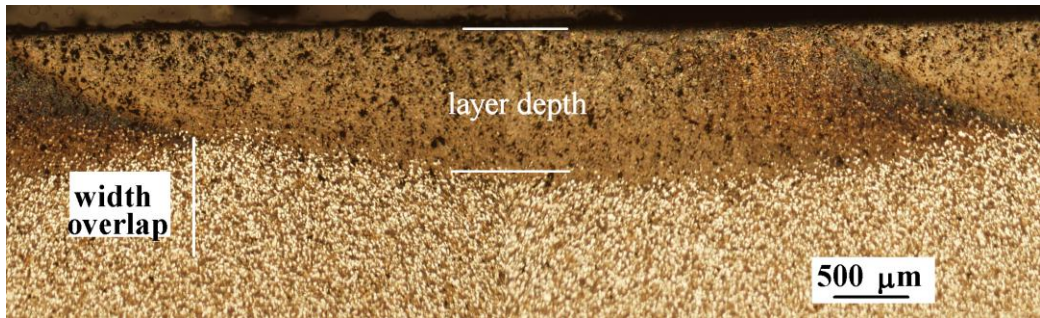


Fig. 3 Macroscopic view of the influence of laser beam on material CrL+0.7 C

As shown in the **Fig. 4a** with increasing rate the depth of penetration decreases, which is basically logical, considering the fact that the higher movement speed of the beam shortens the duration of exposure the beam on the material on the given spot. A more alloyed material has a greater depth of penetration. At the same carbon content, it is the chromium and molybdenum, which improves hardenability. **Fig. 4b** shows the depth of through-hardening (the area in which the value of micro-hardness is $> 500 \text{ HV}0.05$).

Thermal influence in this area is associated with higher crossing the transition temperature than it is usual by classical heat treatment. Here, the crossing of solidus curve may occur. In any case, the subsequent cooling is relatively fast because the heated area is of small volume, by influence of thermal conductivity, heat moves to cooler areas of the non-affected volume. In our case, cooling rate was increased by the influence of flowing argon, which was used to protect against corrosion at high temperatures. Due to the cooling rate, subsequently the transformation of austenite to pearlite, or in accordance with the transformation diagrams [16,17] transformation to martensite or bainite, respectively accumulation of both occurs. In extreme cases, accumulation of all three structures may take place.

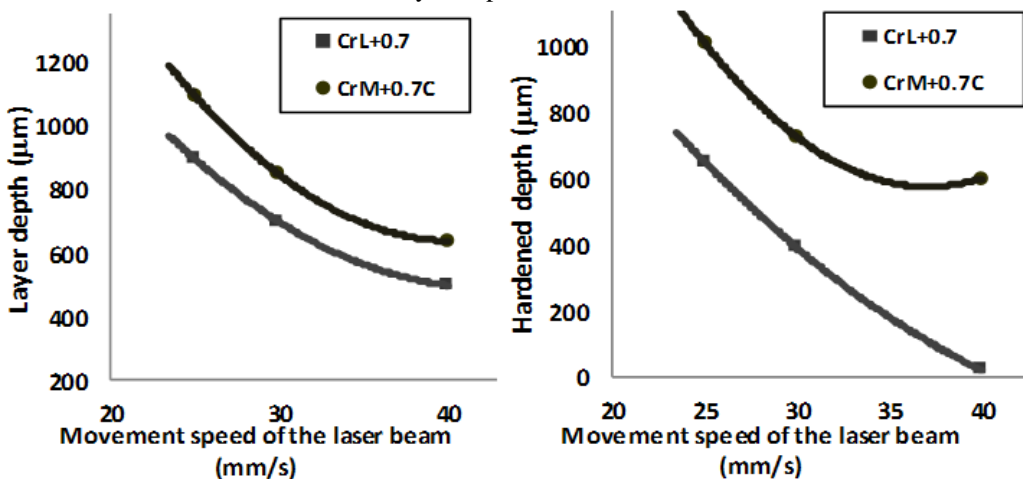


Fig.4 Effect of laser-beam speed a - on the depth of penetration into the material and b – on hardened depth

Except the described structural changes options, in the metallographic analysis we also observed the crossing of the solidus curve, which is demonstrated by surface partially melting. It has the

same shape as the whole affected area. However, it is much shorter and its depth is also reduced. With material CrL +0.7 C at a rate of movement of the beam 25 mm/s melting depth was of about 100 μm on about 700 μm in width. At the remaining two speeds, melting was not observed. Melting by the material CrM +0.7 C was observed to a depth of about 250 μm in width about 3000 μm . At a speed of 30 mm/s very low melting of several μm in depth and width of about 100 μm was observed. After cooling, in the melted place was the dendritic structure of martensite nature created – **Figs. 5, 6**.

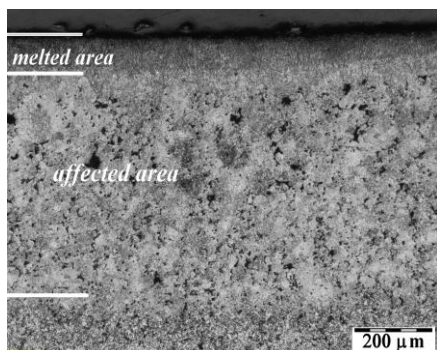


Fig.5 Melted area by CrM+0.7C

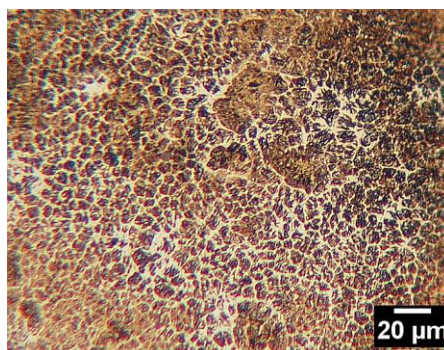


Fig.6 Dendritic structure on surface CrL+0.7C

The easiest and quickest way to find what kind of transformation might occur in this way of heat treatment is the measurement of hardness and its comparison with the hardness of sintered state. Literature references, e.g. [19] are for steel type CrL +0.7% C micro-hardness give the following values: pearlite 300-500, bainite 350-700, martensite 950-1050 HV0.05, resulting from the different transformation temperatures. At CrM steel these values, depending on the cooling rate, are somewhat higher. With this increase martensite hardness of about 100 HV 0.05 units - which is about 10%. The same is true in the case of bainite. In both cases, however, depends on the hardness of the cooling rate. In our case, we used both a method to measure hardness of HV 10 and HV 0.05 on the surface - **Table 2** and also measure the microhardness HV 0.05 for cross-sectional samples. The metallographic structural analysis served as an evidence of the achievements of hardness.

Table 2 The Hardness of the investigated materials after laser hardening

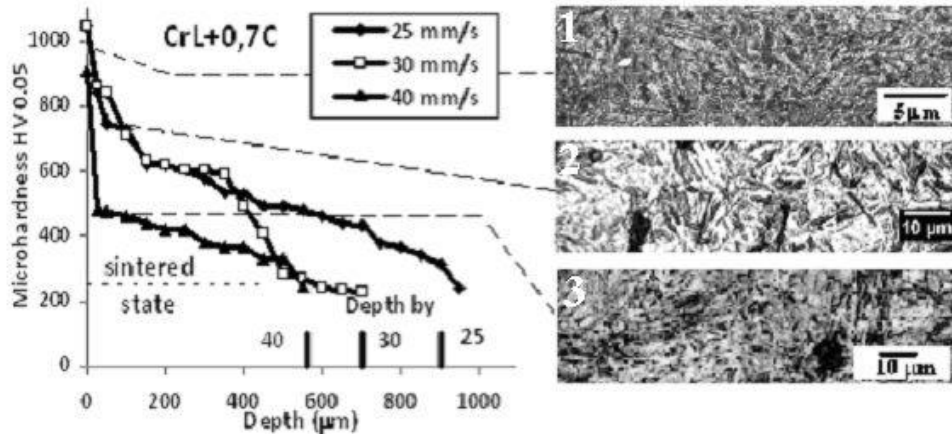
Material	CrL+0.7C			CrM+0.7C		
	25 mm/s	30mm/s	40 mm/s	25 mm/s	30mm/s	40 mm/s
HV10	573	523	400	729	600	550
HV0,05	1000	1000	911	1100	1100	1043

HV10 - measured on the surface HV0,05 - measured direct on the surface

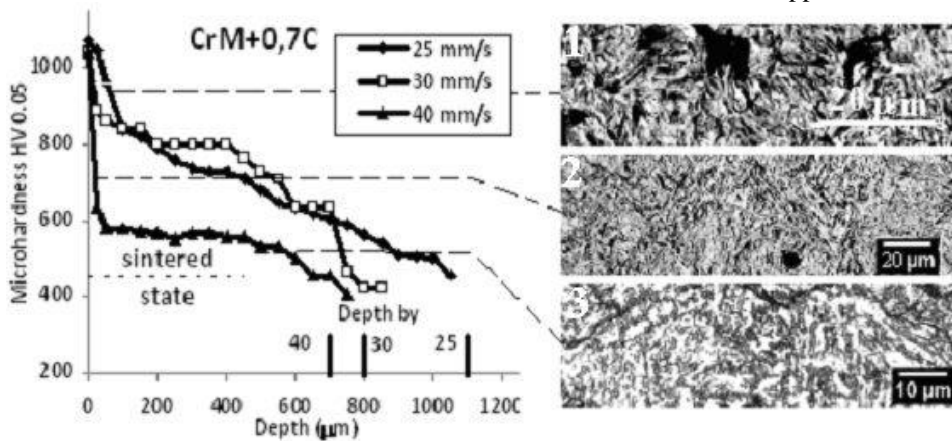
To be able to comment the results shown in Table 2, it is first necessary to specify the value of the measurement of microhardness the cross section of the material. They are in **Figs. 7 a, b**.

From the results obtained the following facts are apparent. Firstly - on the surface in both materials at all speeds of movement of the beam martensite is formed. The depth of the martensite penetration can be roughly read from the diagram based on the already stated values of its hardness. Maximum values in this chart were however measured directly on the surface. Namely, it is not possible to measure (with microhardness tester) the surface layer - thinner than

20-30 μm on a cross section. Therefore, we chose a method of measuring directly on the surface. It requires (due to the condition of the surface) slow and careful polishing with diamond paste to a state when the indenter imprint is visible and measurable.



1-martensite – 980 HV 0,05; 2 – bainite lower 740 HV 0,05; 3 – bainite upper 448 HV 0,05



1-martensite – 965 HV 0,05; 2 – bainite lower 710 HV 0,05; 3 – bainite upper 510 HV 0,05

Fig. 7a,b Microhardness course in the affected area, depending on the velocity of laser beam for CrL and CrM

Results show that the surface microhardness within a single material at the movement of the beam 25 and 30 mm/s is the same. Significantly lower values of microhardness at a speed of 40 mm/s are given mainly by ferrite content. Of the curves behaviours it is also evident that in the early stages, after the cooling starts, there is a sharp drop in microhardness, which is highest at 40 mm/s. That is logical if we assume that at this speed the inflow of thermal energy is the smallest. Then in this period of time a conversion to ferritic-carbide mixtures takes place.

Higher microhardness by CrM material on the surface is given by the higher content of alloying elements, but mainly by the presence of a thin surface layer of martensite that cannot be etched – **Fig. 8**. As evidence of the existence of this layer, not only the image of the obtained microscopically from the cross section of the material, but also from the surface microhardness measurements made a good service. When having etched this surface, we obtained the result

shown in **Fig. 9**. Based on an earlier observation, we can assume that very rapid cooling from high temperatures leads to the formation of very fine martensite, which in this state cannot be etched. This phenomenon of formation is of very often observed commonly with contact fatigue, especially on gearing in the gearbox [20] or on railway rails.

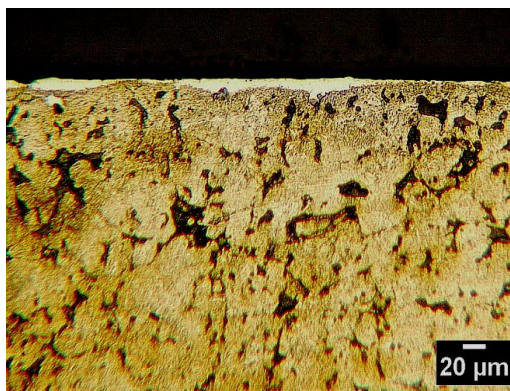


Fig. 8 Martensitic white layer - CrM+0,7C

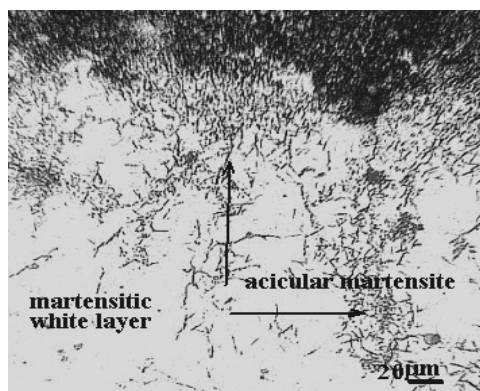


Fig.9 Martensitic white layer + acicular martensite

This is reinforced by the fact that along this layer on the surface there is also martensite, which is of acicular nature. According to the latest research [21], acicular martensite arises under specific conditions. One of requirements that prefer the other authors is a quenching from high temperatures. What in our case is the melted status. Microhardness measurements on the surface of the white areas showed that the hardness is slightly higher than the hardness of acicular martensite. Thus, it is possible that in places where the coating is thinner, after grinding and polishing, we get down to the structure that is underneath. Other authors on the subject of an acicular martensite state [22] that it formed when the carbon content of $> 1\%$. As shown in the cross-sectional observations there were places just below the surface, which showed stronger etchability. We understand that a certain role in this case could be played by paint coating (hot Plasti-Kote paint), by which the sample surface was painted (used in practice due to increased absorption of laser beams and is inherently carbon origin). Heating could by the diffusion effect increase the content of carbon in thin layer on the surface from the original value $0.7\%C$ to the value of more than 1% .

When comparing the results of microhardness with those of the of macro hardness, we can see some disproportions. Firstly, it is necessary to realize that the value macro hardness is a quantity comprising a substantially larger volume of material. Micro-hardness of a CrL material is the highest at speed of 25 mm/s . At this relatively slow movement of the beam, the surface heats up to melting and subsequent rapid cooling are sufficient to create the martensitic structure. Even at a speed of 30 mm/s the martensite is formed at the surface too. Hardness drop in this case is simply caused due to the fact that in the first case, as a consequence of melting, following cooling the material loses its porosity and in the second case the porous material is measured. At the speed of 40 mm/s supply of heat is short - the corresponding speed is lower. In the material a predominantly ferrite-carbide mix is formed - although we have previously argued that martensite is formed on a surface in all cases. However there is difference, when microhardness is measured - there is the possibility to measure the first particle on the surface (size $< 15\text{ }\mu\text{m}$) whereas the indenter penetrates the material at hardness of $1000\text{ HV }0.05$ to the depth of about

4.3 μm . When measuring the macro hardness, the indenter penetrates the material at the same hardness into the depth of about 24 μm . Therefore, the macro hardness is decided by the average of hardness along the depth of indenter penetration into the material. Micro-hardness of CrM material is logically higher applies the same as to material CrL. In the first case the depth of melting is relatively high and hardness corresponds again to the non-porous material with martensitic structure. In the case of a speed of 30 mm/s the surface is melted but only weakly. Thus, even if the structure is martensitic and compact on the surface compact, below it there is a porous material. When measuring hardness, the indenter penetrates down to the porous material. At 40 mm/s, hardness of martensite only of porous material is measured.

It is noted that following laser hardening under the given conditions martensite is always formed on the surface, the thickness of which can be by crude approximation read from the diagrams in Figs. 7a,b. Its appearance is evident from Fig. 1 (in Fig 7a,b) on the right side of the diagram both for the CrL and CrM material. Its hardness can also be measured at a certain depth below the surface. In the areas under the martensite ferritic-carbide structures are formed in accordance with CCT diagrams. In our case it is bainite. Fig. 2 (in Fig.7a,b) in both cases refers to the lower bainite and Fig. 3 (in Figs. 7a,b) to the upper one. In all the six cases, values of microhardness are stated, which were measured in situ following microscopic documentation. It should be noted that the structures after laser hardening are very delicate, and particularly in case of martensite they are difficult to etch. At conventional metallographic magnifications, the details are poorly distinguishable whereas at higher magnifications and their subsequent digitalization the images are less sharp. However, it can ultimately be concluded that our results regarding hardness give sufficient overview of the impact of laser hardening on the properties and thus the potentials for its practical applications.

4 Conclusion

Effect of laser beam on the material produced by powder metallurgy, in its essence, is not different from its impact on the compact materials. Its use on sintered materials (particularly for steel) has many advantages and can successfully replace so called sinterhardening method. Perhaps under certain specific conditions, it can be used in place of some of the classic progressive tightening of the surface layers. There are, however, excluded cases and increase strength properties of the whole volume with well-defined subtle components produced by powder metallurgy.

Regarding the results obtained in our case it can be said to be a quantitatively limited by chemical composition of selected sintered steel, laser device input and selected speeds of laser beam movements. They can be described as follows:

1. Using a laser beam to influence the surface properties of PM materials has proved to be very beneficial. Due to the simplicity and speed of its use as a replacement for traditional methods of heat treatment in some cases indisputable.
2. Achieved values of surface hardness as well as the depth of influence are at least comparable with the type of material studied CrL and CrM with methods cementation or nitriding.
3. Depth of affecting material, which is given by changing the original structure of the constant power laser, depends on the speed of movement of the beam. It decreases as speed increases. Values for CrM material are higher than CrL material. It is due to higher material hardening penetration caused by higher content of Cr and Mo.

4. Changes in the structure led to changes in the values of hardness. It is necessary to distinguish between surface hardness and hardness change on the cross section.
5. In the case of a slower speed of the laser beam, (at constant performance of the laser device) melting of the surface might occur. Slight melting can be beneficial. It has the effect of increasing density in the treated area in terms material density (reduced porosity close to zero), what corresponds to the increase in hardness.
6. The high cooling rate and its correlation with the development of thin high hard very fine martensitic layers can be used in abrasive stress. As an adverse effect one can consider its corresponding fragility, which when under specific load (different forms of fatigue) can initiate cracking and subsequent spread into the material.

References

- [1] P.D. Babu, K. R. Balasubramanian, G. Buvanashakaran: International Journal of Surface Science and Engineering, Vol. 5, 2011, No. 2-3, p. 131-151, DOI: 10.1504/IJSURFSE.2011.041398
- [2] W. Reiter, G. Daurelio, A.D. Ludovico: Proceedings of SPIE - The International Society for Optical Engineering, Vol. 3097, 1997, p. 462-477
- [3] Y. Li, Y. Lu, Y. Liu: Fenmo Yejin Jishu - Powder Metallurgy Technology, Vol. 22, 2004, No. 4, p. 232-235
- [4] V.A. Kovrigin, M.N. Goryushina, S.V. Dubrovskii, B.I. Dudin: Metal Science and Heat Treatment, Vol. 26, 1984, No. 7, p. 513-515, DOI: 10.1007/BF00706707
- [5] R. Bidulsky, M. Actis Grande, J. Bidulska, T. Kvackaj: High Temperature Materials and Processes, Vol. 30, 2011, No. 3, p. 199-203, doi: 10.1515/HTMP.2011.029
- [6] S. So, H. Ki: International Journal of Heat and Mass Transfer, Vol. 61, 2013, No. 1, p. 266-276, DOI: 10.1016/j.ijheatmasstransfer.2013.01.048
- [7] U. Engström: Evaluation of sinterhardening in different PM materials, In: Advances in Powder Metallurgy & Particulate Materials, 2000, New York, p. 5-147 - 5-157
- [8] S. Barnes, M.J. Nash, Y.K. Kwok: Journal of Engineering Materials and Technology, Transactions of the ASME, Vol. 125, 2003, No. 4, p. 372-377
- [9] B. Hu, A. Klekovkin, D. Milligan, U. Engstrom, S. Berg, and B. Maroli: Properties of High Density Cr-Mo Pre-Alloyed Materials High-Temperature Sintered, In: Advances in Powder Metallurgy & Particulate Materials-2004, Vol. 2, Metal Powder Industries Federation, Princeton, 2004, p. 7-28 - 7-40.
- [10] R. Varzel, D. Milligan, U. Engström: Advances In Powder Metallurgy And Particulate Materials, 2007, No.1, p. 5-68 - 5-75
- [11] M. Dlapka, H. Danninger, C. Gierl, H. Altena, G. Stetina, P. Orth: HTM - Haerterei-Technische Mitteilungen, Vol. 67, 2012, No. 2, p. 158-165
- [12] J. Bidulska, R. Bidulsky, M. Actis Grande: Acta Metallurgica Slovaca, Vol. 16, 2010, No. 3, p. 146-150
- [13] R.T. Warzel III, S.H. Luk: International Journal of Powder Metallurgy, Vol. 48, 2012, No. 5, p. 19-22
- [14] D. Rodziňák, V. Zahradníček, P. Hvizdoš, D. Jakubéczyová: Acta Metallurgica Slovaca, Vol. 16, 2010, No. 1, p. 12-19
- [15] D. Rodziňák, P. Hvizdoš, J. Čerňan, K. Semrád: Kovove Materialy, Vol. 50, 2012, No. 5, p. 365-371, DOI: 10.4149/km-2012-5-365

- [16] Y. Yang: Thermodynamic and kinetic behaviours of Aсталoy CrM, Höganäs technical papers AB, SE-263. 83, Höganäs, Sweden, 2000, p. 1-4
- [17] S. Berg, B. Maroli: Properties Obtained by Chromium-containing Material, In: PM²TEC 2002, World Congress on Powder Metallurgy & Particulate Materials in Orlando USA, 2002, p. 1-14
- [18] L. Čiripová, E. Hryha, E. Dudrová, A. Výrostková: Materials and Design, Vol. 35, 2012, p. 619-625, DOI: 10.1016/j.matdes.2011.10.011,
- [19] R. Frykholm, O. Bergman: Chromium Pre-alloyed of PM steels suitable for high performance application, In: PM²TEC 2005, Montreal, Canada, 2005, p. 1-14
- [20] D. Rodziňák: Praktische Metallographie-Practical Metallography, Vol. 27, 1990, No. 6, p. 310-317
- [21] O. D. Sherby, J. Wadsworth, D. R. Lesuer, Ch. K Syn: Materials Transactions, Vol. 49, 2008, No. 9, p. 216-227
- [22] H.-J. Bargel, G. Schulze: Werkstoffkunde, Springer Verlag, Berlin, 2008

Acknowledgment

The authors express thanks to Trumpf Slovakia, GmbH, subsidiary Košice, for allowing us and First Welding company, Inc., Bratislava, for the realization of laser surface treatment on the supplied samples.